J|A|C|S ARTICLES

Published on Web 07/02/2010

Structure and Photoinduced Electron Transfer Dynamics of a Series of Hydrogen-Bonded Supramolecular Complexes Composed of Electron Donors and a Saddle-Distorted Diprotonated Porphyrin

Tatsuhiko Honda,[†] Tatsuaki Nakanishi,[†,||] Kei Ohkubo,[†] Takahiko Kojima,*[,‡] and Shunichi Fukuzumi*[,†,§]

Department of Material and Life Science, Graduate School of Engineering, Osaka University, SORST, Japan Science and Technology Agency (JST), Suita, Osaka 565-0871, Japan, Department of Chemistry, University of Tsukuba, Tsukuba, Ibaraki 305-8571, Japan, and Department of Bioinspired Science, Ewha Womans University, Seoul 120-750, Korea

Received May 7, 2010; E-mail: kojima@chem.tsukuba.ac.jp; fukuzumi@chem.eng.osaka-u.ac.jp

Abstract: The excited-state photodynamics of *intra*supramolecular photoinduced electron transfer was investigated in a series of hydrogen-bonded supramolecular complexes composed of diprotonated 2,3,5,7,8,10,12,13,15,17,18,20-dodecaphenylporphyrin (H_4DPP^{2+}) and electron donors bearing a carboxylate group. The formation of supramolecular complexes was examined by spectroscopic measurements. The binding constants obtained by spectroscopic titration indicate the strong binding (10^8-10^{10} M^{-2}) even in a polar and coordinating solvent, benzonitrile (PhCN). The crystal structure of the supramolecular assembly using ferrocenecarboxylate ($FcCOO^-$) was determined to reveal a new structural motif involving two-point and single-point hydrogen bonding among saddle-distorted H_4DPP^{2+} dication and two $FcCOO^-$ anions. Femtosecond laser flash photolysis was applied to investigate the photodynamics in the hydrogen-bonded supramolecular complexes. Rate constants obtained were evaluated in light of the Marcus theory of electron transfer, allowing us to determine the reorganization energy and the electronic coupling matrix constant of photoinduced electron transfer and back electron transfer to be 0.68 eV and 43 cm^{-1}, respectively. The distance dependence of electron transfer was also examined by using a series of ferrocenecarboxylate derivatives connected by linear phenylene linkers, and the distance dependence of the rate constant of electron transfer (k_{ET}) was determined to be $k_{ET} = k_0 \exp(-\beta r)$, in which $\beta = 0.64$ Å^{-1}.

Introduction

Porphyrin-based artificial photosynthetic systems performing photoinduced energy and electron transfer have extensively been studied and applied to a variety of photofunctional materials[1−9] because the photosynthetic reaction center includes the porphyrin derivatives, i.e., bacteriochlorophylls, which act as a light-harvesting antenna and an electron donor in the electron-transfer cascade. All the components involved in the sequential multistep electron transfer are held in appropriate positions by noncovalent interactions.[10,11] In this context, light-harvesting porphyrin-based supramolecular assemblies built up by noncovalent interactions such as hydrogen bonding[12−21] and electrostatic interaction[22−24] have attracted much attention because of its feasibility, compared to linking them by covalent bonds. However, these interactions are usually weakened in polar solvents, such as acetonitrile and benzonitrile, which can stabilize charge-separated states pro-

[†] Osaka University.
[‡] University of Tsukuba.
[§] Ewha Womans University.
[||] Present address: Advanced Photovoltaics Center, National Institute for Material Science (NIMS), Tsukuba, Ibaraki 305-0047, Japan

(1) (a) Sessler, J. L.; Lawrence, C. M.; Jayawickramarajah, J. *Chem. Soc. Rev.* **2007**, *36*, 314. (b) Sessler, J. L.; Wang, B.; Harriman, A. *J. Am. Chem. Soc.* **1993**, *115*, 10418. (c) Wasielewski, M. R. *Acc. Chem. Res.* **2009**, *42*, 1910. (d) Wasielewski, M. R. *Chem. Rev.* **1992**, *92*, 435.

(2) (a) Gust, D.; Moore, T. A.; Moore, A. L. *Acc. Chem. Res.* **2009**, *42*, 1890. (b) Gust, D.; Moore, T. A.; Moore, A. L. *Acc. Chem. Res.* **2001**, *34*, 40. (c) Gust, D.; Moore, T. A.; Moore, A. L.; Lee, S.-J.; Bittersmann, E.; Luttrull, D. K.; Rehms, A. A.; DeGraziano, J. M.; Ma, X. C.; Gao, F.; Belford, R. E.; Trier, T. T. *Science* **1990**, *248*, 199.

(3) (a) Winters, M. U.; Dahlstedt, E.; Blades, H. E.; Wilson, C. J.; Frampton, M. J.; Anderson, H. L.; Albinsson, B. *J. Am. Chem. Soc.* **2007**, *129*, 4291. (b) Kocherzhenko, A. A.; Patwardhan, A.; Grozema, F. C.; Anderson, H. L.; Siebbeles, L. D. A. *J. Am. Chem. Soc.* **2009**, *131*, 5522. (c) Lovett, J. E.; Hoffmann, M.; Cnossen, A.; Shutter, A. T. J.; Hogben, H. J.; Warren, J. E.; Pascu, S. I.; Kay, C. W. M.; Timmel, C. R.; Anderson, H. L. *J. Am. Chem. Soc.* **2009**, *131*, 13852.

(4) (a) Fukuzumi, S. *Org. Biomol. Chem.* **2003**, *1*, 609. (b) Fukuzumi, S. *Bull. Chem. Soc. Jpn.* **2006**, *79*, 177. (c) Fukuzumi, S. *Phys. Chem. Chem. Phys.* **2008**, *10*, 2283. (d) Ohkubo, K.; Fukuzumi, S. *J. Porphyrins Phthalocyanines* **2008**, *12*, 993. (e) Ohkubo, K.; Fukuzumi, S. *Bull. Chem. Soc. Jpn.* **2009**, *82*, 303.

(5) (a) Asahi, T.; Ohkohchi, M.; Matsusaka, R.; Mataga, N.; Zhang, R. P.; Osuka, A.; Maruyama, K. *J. Am. Chem. Soc.* **1993**, *115*, 5665. (b) Osuka, A.; Noya, G.; Taniguchi, S.; Okada, T.; Nishimura, Y.; Yamazaki, I.; Mataga, N. *Chem.—Eur. J.* **2000**, *6*, 33.

(6) (a) Heitele, H.; Pöllinger, F.; Häberle, T.; Michel-Beyerle, M. E.; Staab, H. A. *J. Phys. Chem.* **1994**, *98*, 7402. (b) Fukuzumi, S.; Ohkubo, K.; Imahori, H.; Shao, J.; Ou, Z.; Zheng, G.; Chen, Y.; Pandey, R. K.; Fujitsuka, M.; Ito, O.; Kadish, K. M. *J. Am. Chem. Soc.* **2001**, *123*, 10676. (c) Hutchison, J. A.; Sintic, P. J.; Brotherhood, P. R.; Scholes, C.; Blake, I. M.; Ghiggino, K. P.; Crossley, M. J. *J. Phys. Chem. C* **2009**, *113*, 11796.

duced by photoinduced electron transfer.[25] Thus, a new strategy to construct stable supramolecular donor−acceptor systems is required for further development of supramolecular photofunctional devices.

Another characteristic of porphyrin, especially for free-base porphyrins (H_2P), is the protonation of the pyrroric nitrogen atoms of the porphyrin ring under acidic conditions to produce diprotonated porphyrin dications (H_4P^{2+}). However, the research on protonated porphyrins has been limited largely to the spectroscopic measurements under strongly acidic conditions because of the low basicity of commonly used planar porphyrins.[26−32] We have developed supramolecular assemblies composed of diprotonated saddle-distorted dodecaphenylporphyrin (H_4DPP^{2+}) based on the high basicity of H_2DPP derived from its deformed structure.[33−35] H_4DPP^{2+} forms hydrogen bonding among the N−H protons of porphyrin and counteranions, such as chloride and carboxylate.[33−35] The H_4DPP^{2+} has been revealed to act as an electron acceptor exhibiting a high reduction potential comparable to those of fullerenes[36] and quinones,[37] whereas free-base porphyrins have normally been used as an electron donor.

A combination of a variety of electron donors with carboxyl groups acting as hydrogen-bonding sites with H_4DPP^{2+} would allow systematic studies on structure and photoinduced electron-transfer dynamics of porphyrin-based electron donor−acceptor supramolecules. We report herein the construction of stable supramolecules composed of H_4DPP^{2+} and electron-donor molecules bearing the carboxylate group in a polar solvent (Scheme 1) and photoinduced electron-transfer dynamics examined by laser flash photolysis and analyzed in light of the

(7) (a) Imahori, H.; Tamaki, K.; Guldi, D. M.; Luo, C.; Fujitsuka, M.; Ito, O.; Sakata, Y.; Fukuzumi, S. *J. Am. Chem. Soc.* **2001**, *123*, 2607. (b) Imahori, H.; Guldi, D. M.; Tamaki, K.; Yoshida, Y.; Luo, C.; Sakata, Y.; Fukuzumi, S. *J. Am. Chem. Soc.* **2001**, *123*, 6617. (c) Imahori, H.; Sekiguchi, Y.; Kashiwagi, Y.; Sato, T.; Araki, Y.; Ito, O.; Yamada, H.; Fukuzumi, S. *Chem.—Eur. J.* **2004**, *10*, 3184.

(8) (a) Ohkubo, K.; Kotani, H.; Shao, J.; Ou, Z.; Kadish, K. M.; Li, G.; Pandey, R. K.; Fujitsuka, M.; Ito, O.; Imahori, H.; Fukuzumi, S. *Angew. Chem., Int. Ed.* **2004**, *43*, 853. (b) Ohkubo, K.; Imahori, H.; Shao, J.; Ou, Z.; Kadish, K. M.; Chen, Y.; Zheng, G.; Pandey, R. K.; Fujitsuka, M.; Ito, O.; Fukuzumi, S. *J. Phys. Chem. A* **2002**, *106*, 10991. (c) Okamoto, K.; Mori, Y.; Yamada, H.; Imahori, H.; Fukuzumi, S. *Chem.—Eur. J.* **2004**, *10*, 474.

(9) (a) Fukuzumi, S.; Kojima, T. *J. Mater. Chem.* **2008**, *18*, 1427. (b) Imahori, H. *J. Mater. Chem.* **2007**, *17*, 31. (c) Dastoor, P. C.; McNeill, C. R.; Frohne, H.; Foster, C. J.; Dean, B.; Fell, C. J.; Belcher, W. J.; Campbell, W. M.; Officer, D. L.; Blake, I. M.; Thordarson, P.; Crossley, M. J.; Hush, N. S.; Reimers, J. R. *J. Phys. Chem. C* **2007**, *111*, 15415. (d) Subbaiyan, N. K.; Wijesinghe, C. A.; D'Souza, F. *J. Am. Chem. Soc.* **2009**, *131*, 14646.

(10) (a) Deisenhofer, J.; Michel, H. *Angew. Chem., Int. Ed. Engl.* **1989**, *28*, 829. (b) von Jagow, G.; Engel, W. D. *Angew. Chem., Int. Ed. Engl.* **1980**, *19*, 659.

(11) Heathcote, P.; Fyfe, P. K.; Jones, M. R. *Trends Biochem. Sci.* **2002**, *27*, 79.

(12) (a) D'Souza, F.; Chitta, R.; Gadde, S.; Rogers, L. M.; Karr, P. A.; Zandler, M. E.; Sandanayaka, A. S. D.; Araki, Y.; Ito, O. *Chem.—Eur. J.* **2007**, *13*, 916. (b) D'Souza, F.; Subbaiyan, N. K.; Xie, Y.; Hill, J. P.; Ariga, K.; Ohkubo, K.; Fukuzumi, S. *J. Am. Chem. Soc.* **2009**, *131*, 16138. (c) D'Souza, F.; Maligaspe, R.; Ohkubo, K.; Zandler, M. E.; Subbaiyan, N. K.; Fukuzumi, S. *J. Am. Chem. Soc.* **2009**, *131*, 8787.

(13) Gadde, S.; Islam, D.-M. S.; Wijesinghe, C. A.; Subbaiyan, N. K.; Zandler, M. E.; Araki, Y.; Ito, O.; D'Souza, F. *J. Phys. Chem. C* **2007**, *111*, 12500.

(14) Hasobe, T.; Kamat, P. V.; Troiani, V.; Solladié, N.; Ahn, T. K.; Kim, S. K.; Kim, D.; Kongkanand, A.; Kuwabata, S.; Fukuzumi, S. *J. Phys. Chem. B* **2005**, *109*, 19.

(15) Saito, K.; Troiani, V.; Qiu, H.; Solladié, N.; Mori, H.; Ohama, M.; Fukuzumi, S. *J. Phys. Chem. C* **2007**, *111*, 1194.

(16) Wessendorf, F.; Gnichwitz, J.-F.; Sarova, G. H.; Hager, K.; Hartnagel, U.; Guldi, D. M.; Hirsch, A. *J. Am. Chem. Soc.* **2007**, *129*, 160579.

(17) Sánchez, L.; Sierra, M.; Martín, N.; Myles, A. J.; Dale, T. J.; Rebek, J., Jr.; Seitz, W.; Guldi, D. M. *Angew. Chem., Int. Ed.* **2006**, *45*, 4637.

(18) (a) D'Souza, F.; Ito, O. *Chem. Commun.* **2009**, 4913. (b) Gadde, S.; Islam, D.-M. S.; Wijesinghe, C. A.; Subbaiyan, N. K.; Zandler, M. E.; Araki, Y.; Ito, O.; D'Souza, F. *J. Phys. Chem. C* **2007**, *111*, 12500. (c) D'Souza, F.; Deviprasad, G. R.; Zandler, M. E.; El-Khouly, M. E.; Fujitsuka, M.; Ito, O. *J. Phys. Chem. A* **2003**, *107*, 4801. (d) Otsuki, J.; Takatsuki, M.; Kaneko, M.; Miwa, H.; Takido, T.; Seno, M.; Okamoto, K.; Imahori, H.; Fujitsuka, M.; Araki, Y.; Ito, O.; Fukuzumi, S. *J. Phys. Chem. A* **2003**, *107*, 379.

(19) (a) Kelley, R. F.; Shin, W. S.; Rybtchinski, B.; Sinks, L. E.; Wasielewski, M. R. *J. Am. Chem. Soc.* **2007**, *129*, 3173. (b) Wilson, T. M.; Hori, T.; Yoon, M.-C.; Aratani, N.; Osuka, A.; Kim, D.; Wasielewski, M. R. *J. Am. Chem. Soc.* **2010**, *132*, 1383.

(20) (a) Sessler, J. L.; Wang, B.; Harriman, A. *J. Am. Chem. Soc.* **1995**, *117*, 704. (b) Sessler, J. L.; Karnas, E.; Kim, S. K.; Ou, Z.; Zhang, M.; Kadish, K. M.; Ohkubo, K.; Fukuzumi, S. *J. Am. Chem. Soc.* **2008**, *130*, 15256. (c) Boul, P. J.; Cho, D.-G.; Rahman, G. M. A.; Marquez, M.; Ou, Z.; Kadish, K. M.; Guldi, D. M.; Sessler, J. L. *J. Am. Chem. Soc.* **2007**, *129*, 5683.

(21) Berman, A.; Izraeli, E. S.; Levanon, H.; Wang, B.; Sessler, J. L. *J. Am. Chem. Soc.* **1995**, *117*, 8252.

(22) (a) Balbinot, D.; Atalick, S.; Guldi, D. M.; Hatzimarinaki, M.; Hirsch, A.; Jux, N. *J. Phys. Chem. B* **2003**, *107*, 13273. (b) Tanaka, M.; Ohkubo, K.; Gros, C. P.; Guilard, R.; Fukuzumi, S. *J. Am. Chem. Soc.* **2006**, *128*, 14625.

(23) Rahman, G. M. A.; Troeger, A.; Sgobba, V.; Guldi, D. M.; Jux, N.; Balbino, D.; Tchoul, M. N.; Ford, W. T.; Mateo-Alonso, A.; Prato, M. *Chem.—Eur. J.* **2008**, *14*, 8837.

(24) (a) Zhang, Y.-M.; Chen, Y.; Yang, Y.; Liu, P.; Liu, Y. *Chem.—Eur. J.* **2009**, *15*, 11333. (b) Takai, A.; Chkounda, M.; Eggenspiller, A.; Gros, C. P.; Lachkar, M.; Barbe, J.-M.; Fukuzumi, S. *J. Am. Chem. Soc.* **2010**, *132*, 4477.

(25) Fukuzumi, S.; Honda, T.; Ohkubo, K.; Kojima, T. *Dalton Trans.* **2009**, 3880.

(26) (a) Karaman, R.; Bruice, T. C. *Inorg. Chem.* **1992**, *31*, 2455. (b) Chirvony, V. S.; van Hoek, A.; Galievsky, V. A.; Sazanovich, I. V.; Schaafsma, T. J.; Holten, D. *J. Phys. Chem. B* **2000**, *104*, 9909.

(27) (a) Senge, M. O.; Forsyth, T. P.; Nguyen, L. T.; Smith, K. M. *Angew. Chem., Int. Ed. Engl.* **1994**, *33*, 2485. (b) Cheng, B.; Munro, O. Q.; Marques, H. M.; Scheidt, W. R. *J. Am. Chem. Soc.* **1997**, *119*, 10732. (c) Gárate-Morales, J. L.; Tham, F. S.; Reed, C. A. *Inorg. Chem.* **2007**, *46*, 1514.

(28) (a) Stone, A.; Fleischer, E. B. *J. Am. Chem. Soc.* **1968**, *90*, 2735. (b) Barakigia, K. M.; Fajer, J. *Acta Crystallogr.* **1995**, *C51*, 511. (c) Medforth, C. J.; Haddad, R. E.; Muzzi, C. M.; Dooley, N. R.; Jaquinod, L.; Shyr, D. C.; Nurco, D. J.; Olmstead, M. M.; Smith, K. M.; Ma, J.-G.; Shelnutt, J. A. *Inorg. Chem.* **2003**, *42*, 2227.

(29) (a) Rosa, A.; Ricciardi, G.; Baerends, E. J.; Romeo, A.; Scolaro, L. M. *J. Phys. Chem. A* **2003**, *107*, 11468. (b) Chen, D.-M.; Liu, X.; He, T.-J.; Liu, F.-C. *Chem. Phys.* **2003**, *289*, 397. (c) Avilov, I. V.; Panarin, A. Y.; Chirvony, V. S. *Chem. Phys. Lett.* **2004**, *389*, 352.

(30) (a) Choi, M. Y.; Pollard, J. A.; Webb, M. A.; McHale, J. L. *J. Am. Chem. Soc.* **2003**, *125*, 810. (b) Okada, S.; Segawa, H. *J. Am. Chem. Soc.* **2003**, *125*, 2792.

(31) (a) Hasobe, T.; Fukuzumi, S.; Kamat, P. V. *J. Am. Chem. Soc.* **2005**, *127*, 11884. (b) Hasobe, T.; Fukuzumi, S.; Kamat, P. V. *J. Phys. Chem. B* **2006**, *110*, 25477. (c) Yoshimoto, S.; Sawaguchi, T. *J. Am. Chem. Soc.* **2008**, *130*, 15944.

(32) (a) Mizuno, Y.; Aida, T.; Yamaguchi, K. *J. Am. Chem. Soc.* **2000**, *122*, 5278. (b) Zhang, Y.; Li, M. X.; Lü, M. Y.; Yang, R. H.; Liu, F.; Li, K. A. *J. Phys. Chem. A* **2005**, *109*, 7442. (c) Mammana, A.; D'Urso, A.; Lauceri, R.; Purrello, R. *J. Am. Chem. Soc.* **2007**, *129*, 8062.

(33) (a) Kojima, T.; Nakanishi, T.; Harada, R.; Ohkubo, K.; Yamauchi, S.; Fukuzumi, S. *Chem.—Eur. J.* **2007**, *11*, 8714. (b) Kojima, T.; Honda, T.; Ohkubo, K.; Shiro, M.; Kusukawa, T.; Fukuda, T.; Kobayashi, N.; Fukuzumi, S. *Angew. Chem., Int. Ed.* **2008**, *47*, 6712.

(34) Nakanishi, T.; Ohkubo, K.; Kojima, T.; Fukuzumi, S. *J. Am. Chem. Soc.* **2009**, *131*, 577.

(35) Honda, T.; Kojima, T.; Fukuzumi, S. *Chem. Commun.* **2009**, 4994.

(36) (a) Fukuzumi, S.; Guldi, D. M. *Electron Transfer in Chemistry*; Wiley-VCH: Weinheim, 2001; Vol. 2, p 270. (b) Yang, Y.; Arias, F.; Echegoyen, L.; Chibante, L. P. F.; Flanagan, S.; Robertson, A.; Wilson, L. J. *J. Am. Chem. Soc.* **1995**, *117*, 7801.

(37) (a) Fukuzumi, S.; Nishizawa, N.; Tanaka, T. *J. Org. Chem.* **1984**, *49*, 3571. (b) Fukuzumi, S.; Koumitsu, S.; Hironaka, K; Tanaka, T. *J. Am. Chem. Soc.* **1987**, *109*, 305. (c) Fujita, M.; Fukuzumi, S.; Matsubayashi, G.; Otera, J. *Bull. Chem. Soc. Jpn.* **1996**, *69*, 1107.

Scheme 1

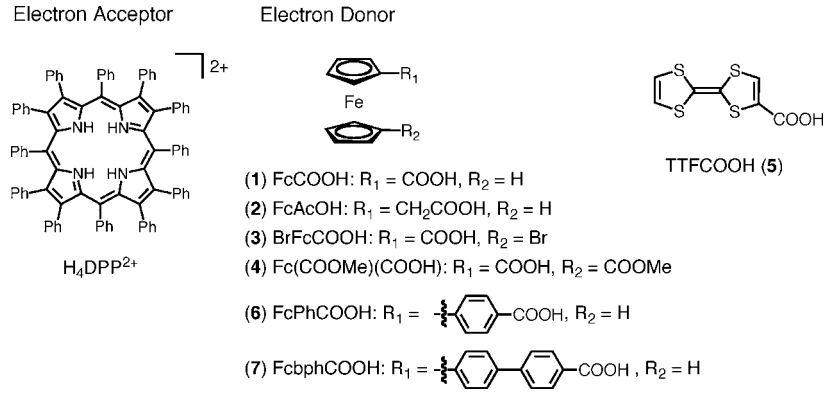

Marcus theory of electron transfer,[38] focusing on the unique characteristics of saddle-distorted diprotonated porphyrin as an electron acceptor in photoinduced intrasupramolecular electron transfer. The distance between the donor and acceptor units was changed systematically by using a series of ferrocenecarboxylate derivatives connected by linear phenylene linkers with H_4DPP^{2+} at different distances. This has enabled us to examine the distance dependence of the rates of photoinduced intrasupramolecular electron transfer for the first time.

Experimental Section

Materials. Chemicals were purchased from commercial sources and used without further purification, unless otherwise noted. Ferrocenecarboxylic acid (FcCOOH, (**1**) in Scheme 1) and ferroceneacetic acid (FcAcOH, (**2**)) were also purchased from commercial sources and used without further purification. Chloroform ($CHCl_3$) and dichloromethane (CH_2Cl_2) used as solvents were distilled over calcium hydride before use. Benzonitrile (PhCN) used for spectroscopic and electrochemical measurements was distilled over phosphorus pentoxide prior to use. H_2DPP,[11] 1-bromo-1′-carboxyferrocene (BrFcCOOH, (**3**)),[40] 1-methoxycarbonyl-1′-carboxyferrocene (Fc(COOMe)(COOH), (**4**)),[41] 2-carboxytetrathiafulvalene (TTFCOOH, (**5**)),[42] and 4-carboxyphenylferrocene (FcPhCOOH, (**6**))[43] were synthesized according to the reported procedures.

Preparation of 4-Methoxycarbonyl-4′-ferrocenylbiphenyl (FcbphCOOMe). A three-necked flask (100 mL) was charged with *p*-bromophenylferrocene (0.3 g, 0.88 mmol),[44] 4-(methoxycarbonyl)phenylboronic acid (0.3 g, 1.76 mmol), tetrakis(triphenylphosphine)palladium(0) (0.1 g, 0.087 mmol), *N*,*N*-dimethylformamide (DMF) (50 mL), water (3 mL), and potassium carbonate (0.2 g, 1.4 mmol). The reaction mixture was heated at 65 °C under nitrogen for 2 h and then cooled to room temperature, after which water was added, and product was extracted with $CHCl_3$. The orange organic layer was washed with water, dried with Na_2SO_4, and filtered. The solvent was removed in vacuo and recrystallized from hot ethanol/water. 4-Methoxycarbonyl-4′-ferrocenylbiphenyl was obtained as orange powder in 34% yield (0.12 g). ^{1}H NMR (300 MHz, $CDCl_3$, 298 K, δ (ppm)): 8.11 (2H, d, J = 8.4 Hz, −ArH), 7.70 (2H, d, J = 8.4 Hz, −ArH), 7.57 (4H, s, −ArH), 4.70 {2H, s, *ortho-H* on (η^5-C_5H_4)}, 4.36 {2H, s, *meta-H* on (η^5-C_5H_4)}, 4.09 (5H, s, η^5-C_5H_5). Anal. calcd for $C_{24}H_{20}FeO_2$: C, 72.74; H, 5.09. Found: C, 72.96; H, 4.97.

Preparation of 4-Carboxy-4′-ferrocenylbiphenyl (FcbphCOOH, (7)). To a solution of FcbphCOOMe (100 mg, 0.25 mmol) in methanol (MeOH) (200 mL) was added potassium hydroxide (50 mg, 0.89 mmol), and the resulting slurry was refluxed for 3 h. After cooling to room temperature, hydrochloric acid (2 mL) and water (200 mL) were added, and resulting precipitates were collected. FcbphCOOH was obtained as yellowish-orange powder in 87% yield (84 mg). ^{1}H NMR (300 MHz, DMSO, 298 K, δ (ppm)): 8.02 (2H, d, J = 8.1 Hz, −ArH), 7.84 (2H, d, J = 8.1 Hz, −ArH), 7.69 (2H, d, J = 8.4 Hz, −ArH), 7.65 (2H, d, J = 8.4 Hz, −ArH), 4.86 {2H, s, *ortho-H* on (η^5-C_5H_4)}, 4.39 {2H, s, *meta-H* on (η^5-C_5H_4)}, 4.04 (5H, s, η^5-C_5H_5). Anal. calcd for $C_{23}H_{18}FeO_2$: C, 72.27; H, 4.75. Found: C, 71.99; H, 4.91.

Preparation of $H_4DPP(FcCOO)_2$. A single crystal of ferrocenecarboxylic acid salt of H_2DPP, $H_4DPP(FcCOO)_2$, was obtained by two-layered recrystallization with addition of CH_3CN on the top of a CH_2Cl_2 solution of H_2DPP (50 mg, 0.041 mmol) and FcCOOH (50 mg, 0.22 mmol). Yield: 36 mg, 52%. Anal. calcd for $H_4DPP(FcCOO)_2(H_2O)(CH_2Cl_2)$ ($C_{115}H_{86}N_4O_5Cl_2Fe_2$): C, 77.31; H, 4.85; N, 3.14. Found: C, 77.44; H, 4.90; N, 3.15.

X-ray Crystallographic Measurements for $H_4DPP(FcCOO)_2$. A single crystal of $H_4DPP(FcCOO)_2$ was mounted on a glass capillary with silicon grease. All measurements were performed on a Rigaku Mercury CCD area detector at −150 °C with graphite-monochromated Mo Kα radiation (λ = 0.71070 Å) up to $2\theta_{max}$ = 54.7°. All calculations were performed using the Crystal Structure crystallographic software package,[45] and structure refinements were made by a direct method using SIR2004.[46] Crystallographic data are summarized in Table 1. Flack parameter was obtained as 0.535(17) by using 7043 Friedel pairs[47] due to the twining of the crystal.

Spectroscopic Measurements. UV−vis spectroscopy was carried out on a Hewlett-Packerd HP8453 diode array spectrometer at room temperature using 1 cm cells. The stoichiometry of formation of the supramolecules was determined through Job's continuous variation experiments,[48,49] where solutions with various H_2DPP/electron donor (DCOOH) molar ratios were prepared while keeping the total molarity of H_2DPP and DCOOH constant. Under these conditions, the stoichiometry of the complex is obtained from the abscissa at the maximum in the Job's plot, whose (x; y) values are given by eqs 1 and 2, where $[H_2DPP]_0$ and $[DCOOH]_0$ denote the initial concentration of H_2DPP and DCOOH, respectively; A is

(38) (a) Marcus, R. A.; Sutin, N. *Biochim. Biophys. Acta* **1985**, *811*, 265. (b) Marcus, R. A. *Angew. Chem., Int. Ed. Engl.* **1993**, *32*, 1111.
(39) (a) Chan, K. S.; Zhou, X.; Luo, B.-S.; Mak, T. C. W. *J. Chem. Soc., Chem. Commun.* **1995**, 733. (b) Liu, C.-J.; Yu, W.-Y.; Peng, S.-M.; Mak, T. C. W.; Che, C.-M. *J. Chem. Soc., Dalton Trans.* **1998**, 1805.
(40) Lai, L.-L.; Dong, T.-Y. *J. Chem. Soc., Chem. Commun.* **1994**, 2347.
(41) Lin, N.-T.; Lin, S.-Y.; Lee, S.-L.; Chen, C.-H.; Hsu, C.-H.; Hwang, L. P. *Angew. Chem., Int. Ed.* **2007**, *46*, 4481.
(42) Green, D. C. *J. Org. Chem.* **1979**, *44*, 1476.
(43) Savage, D.; Gallagher, J. F.; Ida, Y.; Kenny, P. T. M. *Inorg. Chem. Commun.* **2002**, 1034.
(44) Fleckensteina, C. A.; Plenioa, H. *Adv. Synth. Catal.* **2006**, *348*, 1058.
(45) CrystalStructure 3.8.2: Crystal Structure Analysis Package; Rigaku and Rigaku/MSC: The Woodlands, TX, 2000−2008.
(46) Burla, M. C.; Caliandro, R.; Camalli, M.; Carrozzini, B.; Cascarano, G. L.; De Caro, L.; Giacovazzo, C.; Polidori, G.; Spagna, R. *J. Appl. Crystallogr.* **2005**, *38*, 381.
(47) Flack, H. D. *Acta Crystallogr.* **1983**, *A39*, 876.
(48) Job, P. *Ann. Chim. (Paris)* **1928**, *9*, 113.
(49) Hisose, K. *J. Inclusion Phenom. Macrocyclic Chem.* **2001**, *39*, 193.

Table 1. X-ray Crystallographic Data for $H_4DPP(FcCOO)_2$

compound	$H_4DPP(FcCOO)_2$
formula	$C_{119}H_{84}Cl_2Fe_2N_6O_4$
formula weight	1844.53
crystal system	orthorhombic
space group	$P2_12_12_1$ (#19)
T, K	123
α, Å	15.3688(5)
β, Å	23.8539(10)
γ, Å	24.8502(10)
V, Å^3	9110.2(6)
Z	4
no. of reflections measured	73 157
no. of observations	15 493
no. of parameters refined	1154
R_1[a]	0.0693 ($I > 2\sigma(I)$)
R_w[b,c]	0.1922 (all data)
GOF	1.061

[a] $R_1 = \Sigma\ ||F_o| - |F_c||/\Sigma\ |F_o|$. [b] $R_w = [\Sigma(\omega(F_o^2 - F_c^2)^2)/\Sigma\omega(F_o^2)^2]^{1/2}$. [c] $\omega = 1/[\sigma^2(F_o^2) + (0.0500P)^2 + 30.0000P$, where $P = (\max(F_o^2, 0) + 2F_c^2)/3$.

observed absorbance; and $\varepsilon(H_2DPP)$ and $\varepsilon(DCOOH)$ are the molar absorbance coefficients of H_2DPP and DCOOH, respectively.

$$x = [H_2DPP]_0/([H_2DPP]_0 + [DCOOH]_0) \quad (1)$$

$$y = A - \varepsilon(H_2DPP)\cdot[H_2DPP]_0 - \varepsilon(DCOOH)\cdot[DCOOH]_0 \quad (2)$$

A one-step binding model with a 1:2 stoichiometry (eq 3) affords eq 4 (see the derivation in Supporting Information), and A_0 and A_∞ are absorbance of H_2DPP and $H_4DPP(DCOO)_2$, respectively.

$$H_2DPP + 2DCOOH \overset{K}{\rightleftharpoons} H_4DPP(DCOO)_2 \quad (3)$$

$$(A - A_0)/(A_\infty - A) = K([DCOOH] - 2\alpha[H_2DPP]_0)^2,\ \alpha = (A - A_0)/(A_\infty - A_0) \quad (4)$$

The binding constants were determined by UV−vis absorption titrations using eq 4. UV−vis absorption titrations were performed by adding DCOOH into the quartz cell that contained an H_2DPP solution (2.0 mL) by means of a Hamilton syringe. The UV−vis spectra recorded during the titrations were corrected for dilution.

^{1}H NMR spectra were recorded on a JEOL A-300 spectrometer, and chemical shifts were determined relative to the residual solvent peaks. The fluorescence spectra were measured by using an absolute PL quantum yield measurement system (Hamamatsu photonics Co., Ltd., C9920-02) by excitation at 430 nm.

Time-Resolved Transient Absorption Measurements. Femtosecond transient absorption measurements were conducted in deaerated PhCN using an ultrafast source, Integra-C (Quantronix Corp.); an optical parametric amplifier, TOPAS (Light Conversion Ltd.); and a commercially available optical detection system, Helios provided by Ultrafast Systems LLC. The source for the pump and probe pulses was derived from the fundamental output of Integra-C (780 nm, 2 mJ/pulse and fwhm = 130 fs) at a repetition rate of 1 kHz. 75% of the fundamental output of the laser was introduced into TOPAS which has optical frequency mixers resulting in tunable range from 285 to 1660 nm, while the rest of the output was used for white light generation. Prior to generating the probe continuum, a variable neutral density filter was inserted in the path to generate stable continuum, and then the laser pulse was fed to a delay line that provides an experimental time window of 3.2 ns with a maximum step resolution of 7 fs. In our experiments, a wavelength at 430 nm of TOPAS output, which is the fourth harmonic of signal or idler pulses, was chosen as the pump beam. As this TOPAS output consists of not only desirable wavelength but also unnecessary wavelengths, the latter was deviated using a wedge prism with wedge angle of 18°. The desirable beam was irradiated at the sample cell with a spot size of 1 mm diameter where it was merged with the white probe pulse in a close angle (<10°). The probe beam after passing through the 2 mm sample cell was focused on a fiber optic cable that was connected to a CCD spectrograph for recording the time-resolved spectra (410−800, 800−1650 nm). Typically, 2500 excitation pulses were averaged for 5 s to obtain the transient spectrum at a set delay time. Kinetic traces at appropriate wavelengths were assembled from the time-resolved spectral data.

Nanosecond time-resolved transient absorption measurements were performed using a laser system provided by UNISOKU Co., Ltd. Measurements of nanosecond transient absorption spectra were performed according to the following procedure. A deaerated solution was excited by a Panther optical parametric oscillator pumped by a Nd:YAG laser (Continuum, SLII-10, 4−6 ns fwhm) at $\lambda = 430$ nm. The photodynamics was monitored by continuous exposure to a xenon lamp (150 W) as a probe light and a photomultiplier tube (Hamamatsu 2949) as a detector.

Electrochemical Measurements. Measurements of cyclic voltammetry (CV) and differential pulse voltammetry (DPV) were performed on an ALS 630B electrochemical analyzer and measured in deaerated PhCN containing 0.1 M [(n-butyl)$_4$N]PF_6 ($TBAPF_6$) as a supporting electrolyte at room temperature. A conventional three-electrode cell was used with a platinum working electrode (surface area of 0.3 mm^2) and a platinum wire as the counter electrode. The Pt working electrode (BAS) was routinely polished with BAS polishing alumina suspension and rinsed with acetone before use. The potentials were measured with respect to the Ag/$AgNO_3$ (0.01 M) reference electrode. All potentials (vs Ag/Ag^+) were converted to values vs SCE by adding 0.29 V.[50] All electrochemical measurements were carried out under an atmospheric pressure of nitrogen.

Theoretical Calculations. Density functional theory (DFT)[51] calculations were performed with Gaussian03 (Revision C.02, Gaussian, Inc.).[52] DFT calculations on $H_4DPP(FcCOO)_2$ were performed on a 32-processor QuantumCube at the B3LYP/6-31G(d) level of theory. Graphical outputs of the computational results were generated with the Gauss View software program (ver. 3.09) developed by Semichem, Inc.[53]

Results and Discussion

Crystal Structure of $H_4DPP(FcCOO)_2$. A single crystal of the ferrocenecarboxylic acid (FcCOOH) salt of H_2DPP, $H_4DPP(FcCOO)_2$, was obtained by two-layered recrystallization with addition of CH_3CN on the top of a CH_2Cl_2 solution of H_2DPP in the presence of an excess amount of FcCOOH. The X-ray crystal structure of $H_4DPP(FcCOO)_2$ is shown in Figure 1. In the crystal of $H_4DPP(FcCOO)_2$, H_4DPP^{2+} and two ferrocenecarboxylate ($FcCOO^-$) anions were hydrogen-bonded asymmetrically: on one side, the saddle-distorted H_4DPP^{2+} forms two-point hydrogen bonding among two of the N−H protons of pyrroles and two of the oxygen atoms in the carboxylate of $FcCOO^-$ with the interatomic (N···O) distance of 2.726 (5) and 2.587 (4) Å. On the other side, one of the oxygen atoms of the carboxylate in $FcCOO^-$ is hydrogen bonded with two of the N−H protons of pyrroles, showing the interatomic distance of 2.773 (4) and 2.763 (5) Å as shown in Figure S1 (Supporting Information). Both $FcCOO^-$ anions were placed in a cleft formed by the two phenyl groups attached to a pyrrole tilted

(50) Mann, C. K.; Barnes, K. K. *Electrochemical Reactions in Non-aqueous Systems*; Mercel Dekker: New York, 1970.
(51) (a) Becke, A. D. *J. Chem. Phys.* **1993**, *98*, 5648. (b) Lee, C; Yang, W.; Parr, R. G. *Phys. Rev. B* **1988**, *37*, 785.
(52) Frisch, M. J.; et al. *Gaussian 03*; Gaussian, Inc.: Wallingford, CT, 2004. The full reference is given in the Supporting Information.
(53) Dennington, R., II; Keith, T.; Millam, J.; Eppinnett, K.; Hovell. W. L.; Gilliland, R. *GaussView*; Semichem, Inc.: Shawnee Mission, KS, 2003.

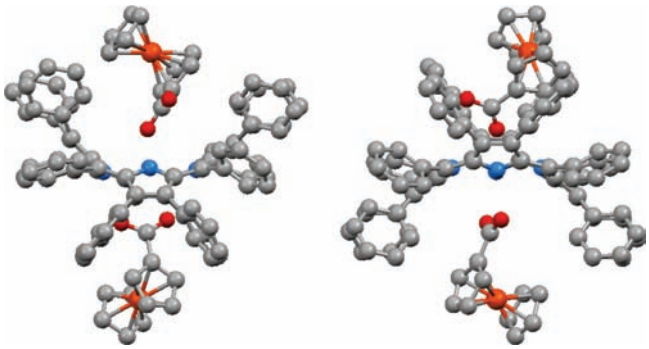

Figure 1. Crystal structure of $H_4DPP(FcCOO)_2$ from different directions. Gray, carbon; blue, nitrogen; red, oxygen; orange, iron. Hydrogen atoms and solvent molecules are omitted for clarity.

up toward the ferrocene parts, forming CH/π interactions with the phenyl groups. Hydrogen bonding between carboxylate and pyrrolic N−H has so far been reported in the crystal structures of diprotonated porphyrins, in which either a one- or two-point hydrogen-bonding mode was observed.[27,28,32a] To the best of our knowledge, this is the first example for the asymmetric hydrogen bonding mode in the crystal structure of protonated porphyrins, which may result from the steric hindrance among the congested peripheral phenyl groups of the porphyrin and the ferrocene moieties. A packing view of $H_4DPP(FcCOO)_2$ was depicted in Figure S2 (Supporting Information). The H_4DPP^{2+} units exhibit intermolecular CH/π interactions among the peripheral phenyl groups. Unlike *the porphyrin nanochannel* having two independent channels in the monoclinic space group of *C*2/c, whose scaffold is composed of H_4DPPCl_2 and two acetonitrile (MeCN) molecules,[33a] no specific supramolecular structure was observed in the packing structure of $H_4DPP(FcCOO)_2$. The asymmetric space group of $P2_12_12_1$ in the crystal of $H_4DPP(FcCOO)_2$ was assumed to be derived from the asymmetric hydrogen-bonding mode of $FcCOO^-$.

Spectroscopic Studies in Solution. To examine formation of supramolecular assemblies in solution, UV−vis titration was carried out by addition of FcCOOH to a benzonitrile (PhCN) solution of H_2DPP as shown in Figure 2(a). Upon addition of FcCOOH, the Soret band of H_2DPP was red-shifted, and its Q-band feature was remarkably changed, which was attributed to formation of diprotonated H_2DPP to produce H_4DPP^{2+}. In our previous work, the use of sulfonic acid resulted in two-step protonation of H_2DPP in PhCN, whereas one-step diprotonation occurred with use of a carboxylic acid.[35] This difference is ascribed to formation of the hydrogen bonds among N−H protons of pyrroles and carboxylates in solution, which facilitates diprotonation of H_2DPP in contrast to the case of sulfonic acid.[35] The observed one-step spectral change in the course of the titration with FcCOOH suggests formation of the hydrogen bonding in solution, as observed in the crystal. Since the spectral change continued up to the addition of more than 2 equiv of FcCOOH, we carried out the continuous variation method[48,49] to determine the stoichiometric ratio between H_2DPP and FcCOOH. Figure 2(b) shows the Job's plot for H_2DPP and FcCOOH, in which the function y (see Experimental Section) is plotted against the molar fraction of H_2DPP. The maximum observed at $x = 0.33$ clearly indicates a 1:2 stoichiometry for the reaction of H_2DPP and FcCOOH. We determined the formation constant of the supramolecule, K, to be 9.2×10^8 M^{-2} from the slope of the linear plot obtained by the titration in Figure S3 (Supporting Information). We also performed UV−vis titrations for the other donor molecules having carboxylate moieties in PhCN to determine binding constants as summarized in Table 2. The binding constants obtained are smaller than those reported in the previous work on hydrogen-bonding supramolecules composed of H_4DPP^{2+} and anthracene derivatives.[35] This is ascribed to larger pK_a values of ferrocene derivatives than the anthracene derivatives, probably due to the negatively charged cyclopentadienyl ring giving rise to destabilization of the carboxylate anion[54] and also steric hindrance between the porphyrin and donor molecules as mentioned above.

We also conducted ^1H NMR titrations in $CDCl_3$ to investigate formation of the supramolecular assemblies. The ^1H NMR spectral change in the course of the addition of FcCOOH is shown in Figure 3. By adding up to 2 equiv of FcCOOH, peaks assigned to *meso*-phenyl protons of H_4DPP^{2+} were all downfield-shifted, indicating formation of H_4DPP^{2+}.[33,35,55] No further shift was observed by addition of more than 2 equiv of FcCOOH. On the contrary, signals of the ferrocene moiety exhibited upfield shifts due to shielding by the ring current of the porphyrin ring upon addition of an increasing amount of FcCOOH (Figure 3). The largest upfield shift was observed on the proton adjacent to the carboxylate, indicating formation of hydrogen bonding between pyrrole moieties and the carboxylate group of $FcCOO^-$ in $CDCl_3$. No further spectral change observed by addition of more than 2 equiv of FcCOOH indicates the stronger binding of $FcCOO^-$ to H_4DPP^{2+} in $CDCl_3$ than that in more polar benzonitrile as mentioned above. Unlike the crystal structure, we could not observe the asymmetrical hydrogen bonding in the ^1H NMR measurements, probably because of the fast exchange of $FcCOO^-$ in the NMR time scale. These observations were common for other donor molecules (Figure S10, Supporting Information).

Electrochemical Measurements. Electrochemical studies using cyclic voltammetry (CV) and differential pulse voltammetry (DPV) were performed to determine the oxidation and reduction potentials of the supramolecular complexes in deaerated PhCN containing 0.1 M $TBAPF_6$ at room temperature. CVs and DPVs were measured for FcCOOH (Figure S11(a), Supporting Information) and the mixture of H_2DPP (1.7 mM) and an excess amount of FcCOOH (4.5 mM) (Figure S11(b), Supporting Information) to obtain the supramolecular complex ($H_4DPP(FcCOO)_2$) in PhCN. The one-electron oxidation potential of the ferrocene moiety (E_{ox}) is changed from 0.70 V (vs SCE) in the absence of H_2DPP to 0.48 V after addition of H_2DPP. This negative shift of oxidation potential is attributed to the deprotonation of FcCOOH ($FcCOO^-$) as a result of formation of the supramolecular complex, and the difference of the oxidation potential (0.22 V) is consistent with the reported value (0.195 V in acetonitrile/H_2O (v/v 8:2)).[54b] The two-electron reduction potential (E_{red}) ascribed to the H_4DPP^{2+} moiety (H_4DPP^{2+}/H_4DPP) is determined to be −0.55 V by DPV.[33a] We conducted electrochemical measurements for other electron-donor molecules (Figure S12, Supporting Information) under the same conditions. The E_{ox} and E_{red} values thus determined are listed in Table 3. In the case of FcAcOH, Fc(COOMe)(COOH), and TTFCOOH, their oxidation potentials in the supramolecular assemblies were significantly cathodically shifted (by 0.12−0.31 V) with respect to the corresponding

(54) (a) Matsue, T.; Evans, D. H.; Osa, T.; Kobayashi, N. *J. Am. Chem. Soc.* **1985**, *107*, 3411. (b) De Santis, G.; Fabbrizzi, L.; Licchelli, M.; Pallavicini, P. *Inorg. Chim. Acta* **1994**, *225*, 239.
(55) Medfortht, C. J.; Senge, M. O.; Smith, K. M.; Sparks, L. D.; Shelnutt, J. A. *J. Am. Chem. Soc.* **1992**, *114*, 9859.

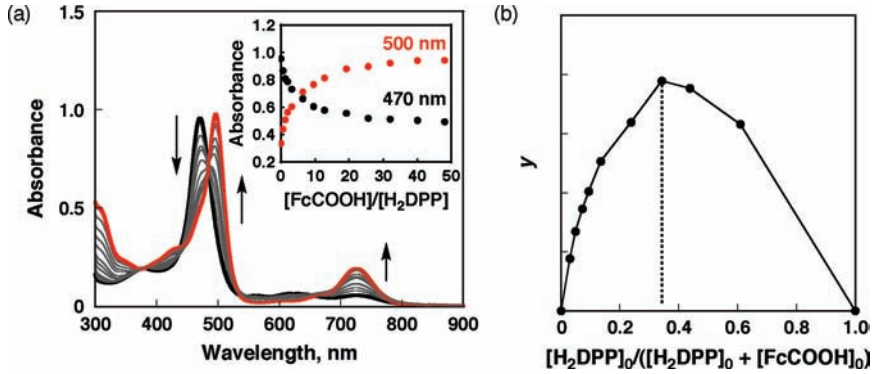

Figure 2. (a) Absorption spectral change in the course of titration of H_2DPP with FcCOOH in PhCN at room temperature. Inset: absorbance change at 470 nm (black line) and 500 nm (red line). (b) Job's continuous variation plot to determine the stoichiometry of the complex formation between H_2DPP and FcCOOH: molar fraction of H_2DPP is varied while keeping the total concentration constant. Dots correspond to absorbance difference (y function, see Experimental Section) at 470 nm for various H_2DPP molar fractions.

Table 2. Formation Constants (K) of H_4DPP^{2+} with Electron Donor

donor molecule	K, M^{-2}
FcCOOH	9.2×10^8
FcAcOH	3.1×10^8
BrFcCOOH	4.6×10^8
Fc(COOMe)(COOH)	6.9×10^9
TTFCOOH	1.9×10^{10}
FcPhCOOH	1.5×10^9
FcbphCOOH	3.5×10^9

carboxylic acids as can be seen in FcCOOH, whereas the oxidation potentials of other electron-donor molecules were slightly changed negatively (by 0.01−0.03 V). The reduction potentials of H_4DPP^{2+} in the presence of an excess amount of the electron-donor molecules having the carboxyl groups were varied in the range of −0.52 to −0.71 V, indicating that the strength of the hydrogen bonding in solution affects the energy of the lowest unoccupied molecular orbital (LUMO) of H_4DPP^{2+}.

Photoinduced Electron Transfer in Hydrogen-Bonding Supramolecules. The fluorescence spectrum of $H_4DPP(FcCOO)_2$ was measured with photoexcitation at 430 nm in PhCN in the presence of an excess amount of FcCOOH to observe weak emission at 814 nm derived from the H_4DPP^{2+} moiety. Fluorescence quenching was observed as reflected in the change in the quantum yields from H_2DPP ($\Phi = 0.85\%$) to $H_4DPP(FcCOO)_2$ ($\Phi = 0.42\%$). The value ($\Phi = 0.42\%$) of the assembly was smaller than that of H_4DPP^{2+}, as observed in the salts of 4-pyridinecarboxylic acid and 2-anthrathene carboxylic acid, which afforded the fluorescence around 800 nm with the quantum yield of approximately 1% (Figure S13, Supporting Information).[33b,35] In addition, fluorescence quenching was also observed using other donor molecules, suggesting that photoinduced electron transfer occurs in the supramolecular assemblies. From the absorption and emission maxima (727 and 814 nm, respectively), the energy of the singlet excited state of H_4DPP^{2+} is determined to be 1.61 eV.

The highest occupied molecular orbital (HOMO) and LUMO of $H_4DPP(FcCOO)_2$ were estimated by DFT calculations using the B3LYP/6-31G(d) basis set on the basis of the crystal structure, indicating that the HOMO and the LUMO are localized on the $FcCOO^-$ moiety and the H_4DPP^{2+} moiety, respectively (Figure 4). The HOMO-1 was also localized on each $FcCOO^-$ moiety, and the energy difference between HOMO and HOMO-1 was small (0.05 eV). This suggests that photoinduced electron transfer occurs from the $FcCOO^-$ moiety to the H_4DPP^{2+} upon photoexcitation of the diprotonated porphyrin.

To examine the photodynamics, time-resolved femtosecond transient absorption spectra of $H_4DPP(FcCOO)_2$ were measured in deaerated PhCN. After laser excitation at 430 nm, the transient absorption bands at 550 and 1030 nm due to the singlet excited state of the H_4DPP^{2+} moiety,$^1[H_4DPP^{2+}]^*$, were observed at 1.5 ps as shown in Figure 5. At 10 ps after photoexcitation, the spectrum changed to that assigned to the electron-transfer state of $H_4DPP(FcCOO)_2$. This assignment was made by the fact that the same absorption bands as those in Figure 5 were observed in the transient absorption spectra in intermolecular photoinduced electron transfer from ferrocene to the triplet excited state of $H_4DPP(4\text{-}PyCOO)_2$ as shown in Figure 6. The transient absorption of the electron-transfer state disappears at 100 ps, and the remaining species was assigned to the triplet excited state of H_4DPP^{2+} by comparison with the transient absorption spectrum of that of $H_4DPP(4\text{-}PyCOO)_2$ (Figure S14(b), Supporting Information). Compared to the nanosecond transient absorption spectrum of the triplet excited state of $H_4DPP(4\text{-}PyCOO)_2$, the observed absorption due to the triplet excited state of $H_4DPP(FcCOO)_2$ was significantly small (Figure S14(a), Supporting Information). Thus, the observed triplet excited state of H_4DPP^{2+} results from the uncomplexed H_4DPP^{2+} without hydrogen-bonded electron donors, judging from the relatively small binding constant in PhCN. From the time profile of the rise and the decay of absorbance at 545 nm depicted in the inset

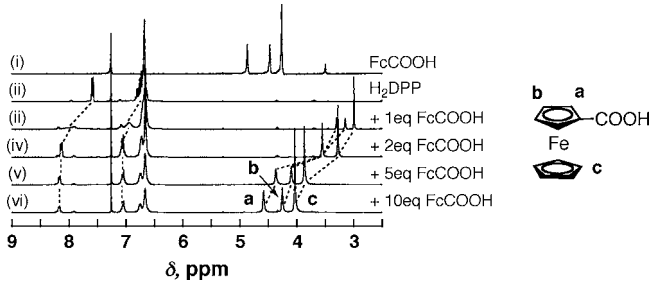

Figure 3. ^1H NMR spectral change of H_2DPP upon addition of FcCOOH in $CDCl_3$ at room temperature. (i) FcCOOH, (ii) H_2DPP, (iii) H_2DPP + 1 equiv of FcCOOH, (iv) H_2DPP + 2 equiv of FcCOOH, (v) H_2DPP + 5 equiv of FcCOOH, and (vi) H_2DPP + 10 eqiuv of FcCOOH.

(56) We could not determine the rate constant of back electron transfer in $H_4DPP(FcbphCOO)_2$ from the decay at 600 nm, in which the remaining components at 3000 ps were assigned as the electron-transfer state (Figure S17, Supporting Information).

Table 3. One-Electron Oxidation Potentials (E_{ox}) of Electron Donors and Reduction Potentials (E_{red}) of H_4DPP^{2+}, Driving Forces of Intrasupramolecular Photoinduced Electron Transfer ($-\Delta G_{ET}$) and Back Electron Transfer ($-\Delta G_{BET}$), and Rate Constants (k_{ET} and k_{BET}) in Supramolecular Complexes of H_4DPP^{2+} with Hydrogen-Bonded Electron Donors in PhCN at Room Temperature

	electron donor	E_{ox}, V[a]	E_{red}, V[a]	$-\Delta G_{ET}$, eV	$-\Delta G_{BET}$, eV	k_{ET}, s^{-1}[b]	k_{BET}, s^{-1}[b]
1	FcCOOH	0.48	−0.55	0.58	1.03	$(5.0 \pm 0.3) \times 10^{11}$	$(6.1 \pm 0.4) \times 10^{10}$
2	FcAcOH	0.35	−0.71	0.55	1.06	$(6.6 \pm 0.3) \times 10^{11}$	$(2.5 \pm 0.1) \times 10^{10}$
3	BrFcCOOH	0.77	−0.52	0.32	1.29	$(1.8 \pm 0.2) \times 10^{11}$	$(2.2 \pm 0.1) \times 10^{10}$
4	Fc(COOMe)(COOH)	0.60	−0.50	0.51	1.10	$(3.8 \pm 0.6) \times 10^{11}$	$(1.6 \pm 0.1) \times 10^{10}$
5	TTFCOOH	0.24	−0.61	0.76	0.85	$(7.4 \pm 0.7) \times 10^{11}$	$(1.8 \pm 0.2) \times 10^{11}$
6	FcPhCOOH	0.53	−0.49	0.59	1.02	$(4.5 \pm 0.5) \times 10^{10}$	$(7.8 \pm 0.5) \times 10^{9}$
7	FcbphCOOH	0.47	−0.50	0.64	0.97	$(2.4 \pm 0.1) \times 10^{9}$	[c]

[a] vs SCE. [b] The rate constants of photoinduced electron transfer (k_{ET}) and back electron transfer (k_{BET}) were determined from both the rise and decay time profile at 545 nm and the binary analysis of the decay time profile at 600 nm. [c] Only the rate constant of intrasupramolecular photoinduced electron transfer could be determined from the decay of absorbance at 540 nm (Figure S15(f) in Supporting Information).[56]

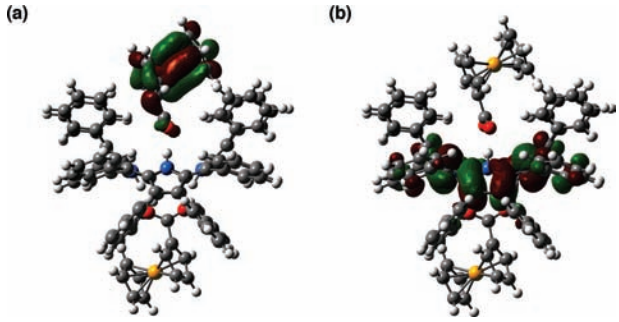

Figure 4. (a) HOMO and (b) LUMO orbitals of $H_4DPP(FcCOO)_2$ calculated by the DFT method at the B3LYP/6-31G(d) level.

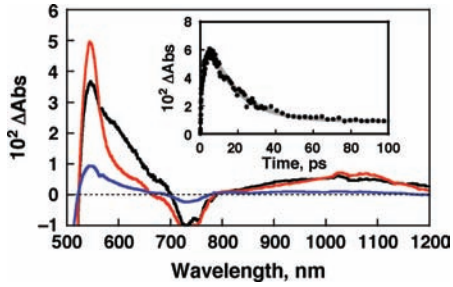

Figure 5. Transient absorption spectra of $H_4DPP(FcCOO)_2$ (20 μM) in PhCN at 1.5 (black), 10 (red), and 100 ps (blue) after femtosecond laser excitation at 430 nm. Inset: A time profile at 545 nm corresponding to intrasupramolecular electron transfer from $FcCOO^-$ to $^1H_4DPP^{2+}$* (rise) and the back electron transfer (decay).

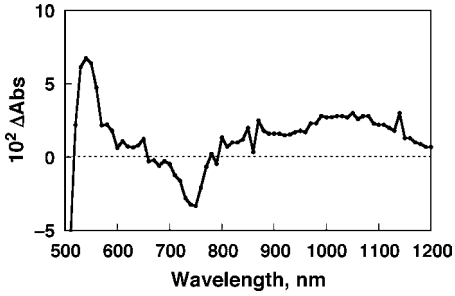

Figure 6. Nanosecond transient absorption spectra of $H_4DPP(4\text{-}PyCOO)_2$ (12 μM) in the presence of ferrocene (1 mM) in PhCN taken at 80 μs after laser excitation at 515 nm.

of Figure 5, we determined the rate constants of photoinduced electron transfer and back electron transfer to be 5.0×10^{11} and 6.1×10^{10} s^{-1}, respectively. The rate constants were also determined for the supramolecules with other electron-donating

Scheme 2. Energy Diagram of Intrasupramolecular Photoinduced Electron Transfer and Back Electron Transfer of Supramolecular Complexes of H_4DPP^{2+} with Hydrogen-Bonded Electron Donors[a]

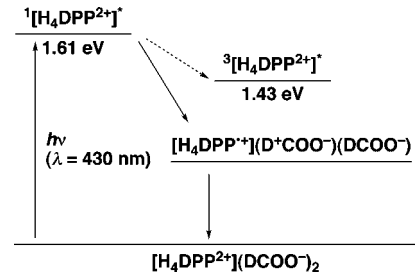

[a] D denotes an electron-donor moiety.

molecules (Figure S15, Supporting Information), and the results are summarized in Table 3 together with the driving forces of photoinduced electron transfer ($-\Delta G_{ET}$, in eV) and back electron transfer ($-\Delta G_{BET}$, in eV). The $-\Delta G_{ET}$ values were determined from the one-electron oxidation potentials of the electron donor moieties (E_{ox}), the reduction potential of the H_4DPP^{2+} moiety (E_{red}), and the energy of the singlet excited state of H_4DPP^{2+} ($^1E^* = 1.61$ eV) using eq 5

$$-\Delta G_{ET} = -e(E_{ox} - E_{red}) + {}^1E^* \quad (5)$$

The $-\Delta G_{BET}$ values were determined using eq 6.

$$-\Delta G_{BET} = e(E_{ox} - E_{red}) \quad (6)$$

The energy diagram of intrasupramolecular photoinduced electron transfer and back electron transfer in hydrogen-bonded supramolecular complexes is depicted in Scheme 2. Intrasupramolecular photoinduced electron transfer occurs from the ground state of an electron donor unit to $^1[H_4DPP^{2+}]^*$, and the back electron transfer affords the ground state of H_4DPP^{2+} rather than the triplet excited state ($^3[H_4DPP^{2+}]^*$) because the energy of the electron-transfer state (0.85−1.29 eV) is lower than that of $^3[H_4DPP^{2+}]^*$ (1.43 eV).[33b,34]

The driving force dependence of the rate constants of intrasupramolecular photoinduced electron transfer from a series of hydrogen-bonded electron donors to $^1[H_4DPP^{2+}]^*$ (k_{ET}) to give rise to the corresponding electron-transfer states and those of back electron transfer to afford the corresponding ground states (k_{BET}) can be analyzed by the Marcus equation of nonadiabatic intramolecular electron transfer (eq 7)[38]

$$k_{ET} = \left(\frac{4\pi^3}{h^2 \lambda k_B T}\right)^{1/2} V^2 \exp\left[-\frac{(\Delta G_{ET} + \lambda)^2}{4\lambda k_B T}\right] \quad (7)$$

where V is the electronic coupling matrix element; h is the Planck constant; T is the absolute temperature; ΔG_{ET} is the free

energy change of electron transfer; and λ is the reorganization energy of electron transfer. The curve fit of the results for a variety of electron donors (**1**−**5** in Table 3) by using eq 7 is shown in Figure 7, affording a small reorganization energy ($\lambda = 0.68 \pm 0.03$ eV) and a large electronic coupling matrix ($V = 43 \pm 7$ cm^{-1}). The λ value is comparable to those of covalently linked donor−acceptor systems consisting of electrically neutral porphyrins as electron donors (0.41−0.66 eV).[6−8] The large electronic coupling matrix may result from the strong interaction between H_4DPP^{2+} and electron-donor molecules because the HOMO of $FcCOO^-$ extends to the carboxylate moiety as shown in Figure 4(a).

The distance dependence of intrasupramolecular photoinduced electron transfer and back electron transfer was also examined by using ferrocenecarboxylic acid derivatives having linear phenylene linker(s) between the ferrocene moiety and the carboxyl group as shown in the inset of Figure 8, where the distance between the electron donor and acceptor is defined as that between the Fe atom of ferrocene and the center of a mean plane of the porphyrin ring of H_4DPP^{2+}, which was obtained from the optimized structure calculated by the DFT calculation at the B3LYP/6-31G(d) basis set (Figure S16, Supporting Information). The distance dependence of the rate constant of intrasupramolecular electron transfer (k_{ET}) is given by eq 8

$$k_{ET} = k_0 \exp(-\beta r) \quad (8)$$

where k_0 is the rate constant of adiabatic intrasupramolecular electron transfer; r is the donor−acceptor center-to-center distance; and β is the decay coefficient factor (damping factor), which depends primarily on the nature of the bridging molecule.[57] From the slope of the plot depicted in Figure 8, the β value was determined to be 0.64 Å^{-1}, which is comparable to those of covalently phenylene-bridged multiporphyrin systems. The distance dependence of the rate constant of back electron transfer (k_{BET}) was also determined to be 0.53 Å^{-1} (Figure S17 in Supporting Information). This indicates that intrasupramolecular photoinduced electron transfer and back electron transfer in supramolecular complexes of H_4DPP^{2+} with hydrogen-bonded electron donors are as efficient as covalently bonded electron-donor systems.[58] To the best of our knowledge, this is the first example of the distance dependence of photoinduced electron transfer in the supramolecular system.

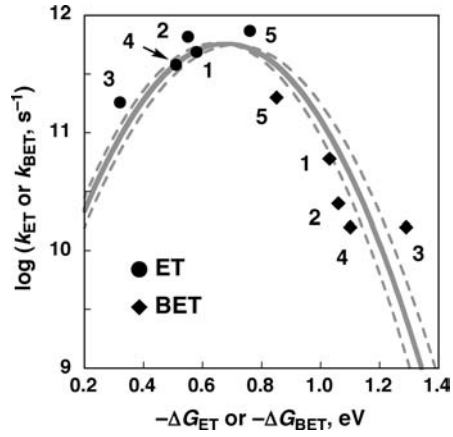

Figure 7. Driving force dependence of log k_{ET} (●) or k_{BET} (◆) for intrasupramolecular photoinduced electron transfer and back electron transfer in supramolecular complexes of H_4DPP^{2+} with hydrogen-bonded electron donors (the numbers correspond to those in Table 3) in PhCN at room temperature. The fitting to the Marcus theory of the electron transfer (eq 7) is shown by the solid line with $\lambda = 0.68$ eV and $V = 43$ cm^{-1} and the dotted lines with $\lambda = 0.65$ and 0.71 eV and $V = 43$ cm^{-1}, respectively.

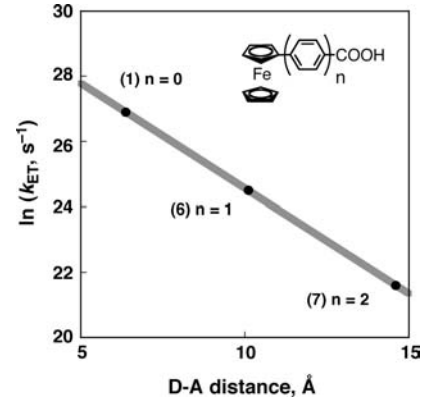

Figure 8. Distance dependence of ln k_{ET} for intrasupramolecular electron transfer from electron donors ((**1**) $FcCOO^-$, (**6**) $FcPhCOO^-$, and (**7**) $FcbphCOO^-$) to $^1[H_4DPP^{2+}]$*, where the distance between an electron donor and an electron acceptor is defined as that between the Fe atom of the ferrocene moiety and the center of a mean plane of the porphyrin ring.

Conclusion

Systematic investigations have been performed on formation of the hydrogen-bonding supramolecular complexes composed of H_4DPP^{2+} and electron donors bearing a carboxylic group and the photodynamics of intrasupramolecular photoinduced electron transfer and back electron transfer. The crystal structure of the supramolecular complex of H_4DPP^{2+} with two $FcCOO^-$ anions has successfully been determined to exhibit asymmetrical hydrogen bonds between the N−H protons of H_4DPP^{2+} and the carboxylate groups of two $FcCOO^-$ anions. Formation of the 1:2 supramolecular complexes between H_4DPP^{2+} with two donor anions was confirmed by spectroscopic measurements, and the formation constants (10^8−10^{10} M^{-2}) were large enough to afford the supramolecular complexes in PhCN. Intrasupramolecular photoinduced electron transfer from the hydrogen-bonded electron donors to $^1[H_4DPP^{2+}]$* was investigated by femtosecond laser flash photolysis. The determined rate constants were evaluated in light of the Marcus theory of electron transfer to afford a small reorganization energy (0.68 eV), indicating intrinsic small structural change of the porphyrin ring upon electron transfer. The distance dependence of the intrasupramolecular photoinduced electron transfer was investigated for the first time by using ferrocenecarboxylic acid derivatives including various lengths of phenylene linkers to determine the damping factor of the rate constant of electron transfer to be 0.64 Å^{-1}. Our results clearly show that the diprotonated dodecaphenylporphyrin acts as a hydrogen-bonding donor in formation of supramolecular complexes with conjugate bases of acids and also an electron acceptor in intrasupramolecular photoinduced electron transfer. The combination of a variety of electron donors with carboxyl groups acting as hydrogen bonding sites with a diprotonated porphyrin (H_4DPP^{2+}) in the present study provides a versatile strategy to construct stable supramolecular electron donor−acceptor systems for further development of supramolecular photofunctional devices.

(57) Closs, G. L.; Miller, J. R. *Science* **1988**, *240*, 440.
(58) (a) Osuka, A.; Maruyama, K.; Mataga, N.; Asahi, T.; Yamazaki, I.; Tamai, N. *J. Am. Chem. Soc.* **1990**, *112*, 4958. (b) Helms, A.; Heiler, D.; McLendon, G. *J. Am. Chem. Soc.* **1992**, *114*, 6221. (c) Pettersson, K.; Wiberg, J.; Ljungdahl, T.; MÅrtensson, J.; Albinsson, B. *J. Phys. Chem. A* **2006**, *110*, 319.

Acknowledgment. This work was supported by Grants-in-Aid (Nos. 21750146 and 20108010), a Global COE program, "the Global Education and Research Center for Bio-Environmental Chemistry" from the Japan Society of Promotion of Science (JSPS), Iketani Science and Technology Foundation, The Ministry of Education, Science, Technology of Japan, and by KOSEF/MEST through WCU project (R31-2008-000-10010-0).

Supporting Information Available: Absorption titration, data of electrochemical measurements, fluorescence spectra, transient absorption spectra, and complete citation details of ref 52. This material is available free of charge via the Internet at http://pubs.acs.org.

JA103889F